

SECTION 27

DETECTION OF OIL SPILLS USING
13.3-GHz RADAR SCATTEROMETER

by

**ORIGINAL CONTAINS
COLOR ILLUSTRATIONS**

K. Krishen
Lockheed Electronics Company, Inc.
Earth Observation Department
Houston, Texas

ABSTRACT

This paper describes the results of an analysis of 13.3-GHz Single Polarized Scatterometer data collected during NASA/MSC Mission 135, flown on March 16, 1970. Data were gathered over a crude oil spill on the Gulf of Mexico (Test Site 128) off the Mississippi Delta. With the aid of RC-8 camera photographs, the scattering cross section was correlated with the extent of the oil spill. The scattering cross section at higher incidence angles (25° to 50°) decreased by 5 dB to 10 dB in the presence of the oil spill. This was attributed to oil's damping of small gravity and capillary waves. The composite scattering theory and the scatterometer acquired data were used to obtain an expression of radar scattering over ocean surfaces with oil spills. The study demonstrates that the presence and extent of oil spills can be detected using high frequency radar systems.

INTRODUCTION

In recent years transportation of crude oil using super tankers and stepped up exploration for oil from ocean drilling towers have increased the possibilities of pollution of oceans from oil spills. The desirability of using remote sensors to detect and monitor oil spills is well recognized. Radar's ability to rapidly search wide areas with high resolution offers global scale monitoring of oil spills. Furthermore, radars operated in the frequency range from UHF to X-band are relatively insensitive to bad weather and cloud cover, and can collect data both night and day. Radar's potential for detection and monitoring of oil spills has been demonstrated in experiments conducted by the Naval Research Laboratory¹ (NRL) utilizing the NRL Four-Frequency System at 0.428 GHz, 1.228 GHz, 4.425 GHz, and 8.91 GHz.

At the request of the U.S. Coast Guard, NASA/MSC flew Mission 135 over the Chevron oil spill on March 16, 1970, with the NASA 927 (Lockheed NP3A) aircraft. The NASA 927 remote sensors used on the flight included

RC-8 cameras and a 13.3-GHz Single Polarized Scatterometer. The purpose of the scatterometer was to obtain the radar signature of the oil-covered ocean surface. Ground truth data for Mission 135 were collected by Coast Guard personnel and oceanographers from Louisiana State University.

This paper describes an analysis of the Mission 135, 13.3-GHz vertical-transmit, vertical-receive scatterometer data. The data were collected simultaneously for incident angles between $+60^\circ$ and -60° using doppler coherent wave techniques. A digital processing program yielded a backscattering cross section (σ_0) versus incident angle (θ) curve for the preceding range of incident angles. In the range of incident angles between 25° and 50° , the scattering cross section decreased 5 dB to 10 dB in the presence of the oil spill. The behavior of σ_0 can be explained by a theoretical composite scattering model. The decrease in scattering cross section in the presence of oil is attributed to the damping by oil of small gravity and capillary waves. This decrease in scattering cross section can be used to locate and monitor the oil spill. Repeated coverage of the affected area and presentation of the scatterometer data on either a two-dimensional matrix printout or a black and white or false color image can be used to monitor the movement of oil slicks.

13.3-GHz SCATTEROMETER DATA

A functional and equipment description of the 13.3-GHz Scatterometer used on Mission 135 is contained in Krishen, et al². In operation the scatterometer's radar energy is radiated by an antenna with a wide fore and aft beam and a narrow transverse beam (see Figure 1). The returned energy may be separated as a function of incidence angle using the doppler equation. Radar cross section per unit area is given by the equation:

$$\sigma(\theta) = \frac{P_R}{P_T} \frac{2(4\pi)^3}{\lambda^3} \cdot \frac{Vh^2}{\Delta f_d} \cdot \frac{1}{\int_{-\psi_1}^{\psi_2} \{G_T(\psi)G_R(\psi)\}_\theta d\psi} \quad (1)$$

where,

P_T = transmitted power

P_R = power received in the doppler window defined by Δf_d

G_T, G_R = transmitting antenna and receiving antenna gain, respectively, as a function of θ (incident angle), and ψ (cross track angle)

h = altitude of the aircraft.

Any altitude, pitch, and velocity perturbations in aircraft parameters are properly reflected in the processing plan. A ferrite modulator is used to calibrate the system by providing an absolute power reference for the transmitted signal.

Statistical averages and variance of $\sigma(\theta)$ also are computed in the computer program, using equation (1) and taking logarithms after averaging is performed. The average values of the scattering cross section are represented by $\sigma_0(\theta)$ and $\sigma_0(\theta)_{dB}$ where,

$$\sigma_0(\theta)_{dB} = 10 \log_{10} (\sigma_0(\theta)) \quad .$$

GROUND TRUTH DATA

The MSC Earth Observations Aircraft Program Mission 135 was conducted over the Chevron drilling platform oil spill on March 16, 1970, from the NASA 927 (NP3A) aircraft. Chevron offshore production platform MP-41C, off the Mississippi Delta, caught fire on February 10, 1970. On March 10 the fire was successfully extinguished, but crude oil continued to spill for approximately 1 month before all wells were capped. Two flights were flown, one during the day and one at night. Figure 2 shows the location of the accident; it is northeast of the Mississippi Delta near the Mississippi River, Gulf outlet channel. The approximate flight lines, as depicted in NASA/MSC Mission 135, Screening and Indexing Report³ are shown in Figure 3.

Ground truth for Mission 135 was taken from the U.S. Coast Guard's (USCG) on-the-scene situation reports and from data gathered by the Louisiana State University (LSU) staff⁴. The U.S. Coast Guard situation reports, summarized in the appendix of the LSU report, outline chronological developments of the Chevron oil spill. The LSU report contains measurements of tides, winds, waves, salinity, temperature and currents. The USCG routine situation reports list direction and approximate width and length of the oil slick when visibility allowed observations from helicopters or other aircraft. Analysis and interpretation of all ground truth data are given in the LSU report.

The scattering cross sections at the 13.3-GHz frequency are dependent on the local wind velocity⁵; therefore, wind velocity and sea state measurements in the oil spill area are needed for interpretation of the scatterometer data. The measurements of sea state and wind velocity⁴ are plotted in Figures 4 and 5. The wind measurements were taken onboard the U.S. Coast Guard Cutter *Dependable* in the vicinity (Figure 2) of Chevron

platform MP-41C. The anemometer height on the *Dependable* is approximately 18.5 meters*. The wave height and wave period measurements were taken from Chevron platform MP-41M (Figure 2). The wind measurements for the same time intervals are given in Figure 5.

The relative direction flown by the NASA 927 aircraft with respect to wind is shown in Figures 6 and 7 for flights 1 and 2, respectively (in these figures F1L10R4 is an abbreviation for Flight 1, Line 10, Run 4).

The extent of oil cover was reported by the U.S. Coast Guard at 1225 hours local time. In summary, USCG reported a major oil slick of approximately 1-1/2 to 2 miles extent approximately 240° true north from the platform, dispersing to medium crude and rainbow slick 3 miles from the rig. The total slick extended 5 miles west, 6 miles north, 3 miles east, and 5 miles south of the rig (Figure 8). Furthermore, USCG reports the slick was well dispersed and areas of medium crude were on the periphery of the total area.

In addition to the ground truth provided in the LSU and USCG reports, photographs were taken by the RC-8 cameras during flight 1. One RC-8 camera was loaded with color film (type SO 397) and the other with color infrared film (type SO 117). Both cameras have a 9 by 9 inch film format and provision for recording time and aircraft attitude and altitude between film frames. The RC-8 field of view is 74° . Photographic coverage was used in this study to correlate scatterometer data with oil covered areas. Identification marks such as MP-41C (Figure 9) and Breton Island (Figure 3) were used to pinpoint the areas over which the aircraft was flying at a particular time. In this paper only typical photographs are presented in reference to scatterometer data interpretation. Analysis of Mission 135 photographic coverage is given in a report by Catoe⁶.

CORRELATION OF 13.3-GHz SCATTEROMETER DATA WITH THE OIL SLICK

Radar backscattering cross sections are dependent upon surface roughness, dielectric properties, and angle of incidence. In the recent past, several experimental and theoretical models have given the relationship between radar backscatter and ocean surface parameters (Wright⁷ and Krishen⁵). In this paper the radar signature of an ocean surface oil slick is studied. In particular, the signature of an oil slick is compared to a sea surface without oil slick. Differences in the scattering cross sections can be utilized to distinguish an oil slick from its background.

*Telephone conversation with S. P. Murray, LSU.

During Mission 135, several runs of scatterometer data were taken. For this analysis, only those data were processed for which the scatterometer signal-to-noise ratio was highest. The results presented in this paper are based on F1L1OR3, F1L1OR4, F1L1R1, F2L1OR1, F2L1OR2, and F2L1OR5 data. Photographic coverage was available only for flight 1.

An area with no significant oil slick (Figure 10) was chosen from ground truth data. The average scattering cross section for this area is given in Figure 11. A comparison of Mission 135 (no significant slick) F1L1OR4 data with F1L1R1 of Mission 119 data for the same wind conditions is also given in Figure 11. Mission 119 was flown over site 86 near Argus Isle, Bermuda, during January and February 1970. Mission 119 was flown over open ocean during fully developed conditions, while Mission 135 was flown over relatively shallow waters near the coast. In view of this, and the fact that only approximate values of wind velocity are available, one can conclude that an agreement between Mission 119 and 135 data exists within experimental error tolerances.

An area where significant oil was present was chosen (Figure 12), and the corresponding scatterometer data was processed. The data for Mission 135, F1L1OR4 with oil slick present, is given in Figure 13, which also shows data from Mission 156 (FCF). Mission 156 (FCF) was flown over the Gulf of Mexico near Galveston, Texas, in relatively calm conditions (5 to 6 knots wind speed) in February 1971. The agreement is striking.

The comparisons shown in Figures 11 and 13 indicate that in the presence of oil, high surface wind velocity ocean radar scattering cross section is similar to that of an ocean with low surface wind speed.

Radar scattering cross sections for ocean surfaces both with and without oil slicks are compared in Figure 14. At higher angles (25° and above) the cross section decreases about 7 dB in the presence of oil. This implies that the power returned from an oil slick is decreased by a ratio of 5 over that returned from an oil-free surface. The data for F1L1OR3 was studied and showed a similar relationship.

Flight 1, line 11, run 1 was flown over an area where no significant oil slick was present. The scattering cross section for this data compared to the data shown in Figure 11 showed close agreement.

Flight 2 was conducted at night; consequently, no photographic data is available. But based on the approximate ground track and ground truth, one can select data from flight 2 for an area relatively free of oil slick and for an oil slick covered area. Flight 2 data compared to flight 1 data showed good agreement. Furthermore, the decrease in scattering cross section at higher angles compares very well (Figure 15) with the results obtained for flight 1 (Figure 14). The results of F2L1OR1 and F2L1OR5

show consistently similar decreases in radar scattering cross section. The feasibility of using radars both day and night for detection and monitoring of oil slicks is thus evident.

If the angle of incidence is kept constant along the flight path, one can generate a graph (Figure 16) of average σ_0 as a function of time/distance. In this graph an average σ_0 for 20-second intervals is plotted. The dip in the graph indicates the presence of oil. Other sets of data over the slick showed similar results.

The behavior of σ_0 can be explained using a theoretical composite scattering model in which the ocean surface is considered a slightly rough surface (high frequency gravity and capillary waves) superimposed on a larger structure (sea waves and swells)⁵. It has often been suggested that near the normal incidence for backscattering cross sections, scattering of the optics type [Kirchhoff method] predominates. In other directions, however, the slight roughness on top of large scale roughness constitutes the major source of scattering. In view of this, Wright⁷ and Guinard and Daley⁸ ignore the large structure effects to account for scattering at higher backscattering angles. Their procedure parallels Rice⁹, Barrick and Peake¹⁰, and Valenzuela¹¹. The presence of a large structure introduces a modification which is small for vertical-transmit, vertical-receive cases (Wright⁷). For Rice's method the backscattering cross sections of a slightly rough surface using first order terms are given by

$$(\sigma_{\lambda\delta})'_s = 4\pi k_0^4 \cos^4 \theta |\alpha_{\lambda\delta}|^2 W(p,q) \quad (2)$$

where,

k_0 = wave number of the incident radar energy

θ = the incident angle

$W(p,q)$ = the roughness spectral density of the surface, and p,q are radian wave numbers

$$\alpha_{HH} = \frac{\epsilon - 1}{\left[\cos \theta + \sqrt{\epsilon - \sin^2 \theta} \right]^2}$$

$$\alpha_{VV} = \frac{(\epsilon - 1)[(\epsilon - 1) \sin^2 \theta + \epsilon]}{\left[\epsilon \cos \theta + \sqrt{\epsilon - \sin^2 \theta} \right]^2}$$

ϵ = the complex dielectric constant of the surface.

To determine the oil slick's effect on the sea surface, the directional spectrum of the sea's small gravity-capillary structure is expressed as

$$W(r) = kr^{-k_3}$$

where,

$$r = \sqrt{p^2 + q^2}.$$

The values of k and k_3 are dependent on the small structure atop the large structure. After substitution of this spectrum and evaluation at the Bragg scattering condition (Wright⁷), equation (2) yields

$$\sigma_0(\theta) = k_1 |\alpha_{vv}|^2 (\cos \theta)^4 (\csc \theta)^{k_3} \quad (3)$$

for the vertical-transmit, vertical-receive polarization combination. In equation (3) k_1 is directly proportional to k . Two sets of data, corresponding to no significant oil slick and significant oil slick, were chosen and the values of k_1 and k_3 sought for best fit. The values of these constants for no significant oil (F1L10R4, from 21:27:26 to 21:27:45 GMT) are

$$k_1 = 0.005118$$

$$k_3 = 5.25.$$

Using these values for the constants, the calculated values compare very well with the experimental results as shown in Figure 17.

In the presence of oil (F1L10R4, from 21:26:26 to 21:26:45 GMT), the spectrum constants were given by

$$k_1 = 0.0003275$$

$$k_3 = 7.0.$$

A comparison of the calculated and experimental values is shown in Figure 18. The results of this study demonstrate that the spectrum of small gravity and capillary waves diminishes significantly in the presence of oil. Cox and Munk¹² measured the mean squared slope in both the presence and absence of oil slicks, and found that the mean squared slope in the presence of oil slicks was about one-third that in the absence of slicks. The oil's smoothing of the sea surface is amply verified by the change in the values of k_1 and k_3 determined in this study.

CONCLUSIONS

The presence of oil spill on a water surface can be detected at 13.3 GHz because of a sharp decrease in scattering cross section (for vertical-receive, vertical-transmit polarizations). The decrease in scattering cross section is attributed to damping of small gravity and capillary waves on the water surface. Repeated coverage of an affected area with radars and presentation of the data as false-color photography can be used to detect and monitor the spread of an oil spill. Further experimentation is needed to establish a relationship between thickness of the oil spill and radar backscattering cross sections.

REFERENCES

1. Guinard, N. W., The Remote Sensing of Oil Slicks, *Proc. Seventh International Sym. of Environment*, The University of Michigan, May 1971.
2. Krishen, K., N. Vlahos, O. Brandt, and G. Graybeal, Results of Scatterometer Systems Analysis for NASA/MSC Earth Observation Sensor Evaluation Program, *Proc. Seventh Int'l. Sym. of Environment*, The University of Michigan, May 1971.
3. NASA/MSC, *Screening and Indexing Report, Mission 135, Site 128*, Manned Spacecraft Center, Houston, Texas, May 1970.
4. Murray, S. P., W. G. Smith, and C. J. Sonu, *Oceanographic Observations and Theoretical Analysis of Oil Slicks During the Chevron Spill*, Tech. Rept. No. 87, Louisiana State University, September 1970.
5. Krishen, K., Correlation of Radar Backscattering Cross Sections with Ocean Wave Height and Wind Velocity, *Journal of Geophy. Res.*, 76, No. 27, 6528-6539, 1971.
6. Catoe, C. E., *Results of Chevron Oil Spill in Gulf of Mexico, Final Rept.*, Project 714104/A/004, U.S. Coast Guard, Washington, May 1970.
7. Wright, J. W., A New Model for Sea Clutter, *IEEE Trans. Antennas Propagat.*, AP-16, 217-223, 1968.
8. Guinard, N. W., and J. C. Daley, An Experimental Study of a Sea Clutter Model, *Proc. IEEE*, 58, 543-550, 1970.
9. Rice, S. O., *Reflection of Electromagnetic Waves by Slightly Rough Surfaces: The Theory of Electromagnetic Waves* (a symposium), Interscience, New York, 1951.
10. Barrick, D. E., and W. H. Peake, Scatterning from Surface with Different Roughness Scales: Analysis and Interpretation, *Res. Rep. BAT-197A-10-3*, Batelle Memorial Institute, Columbus, Ohio, 1967.
11. Valenzuela, G. R., Depolarization of EM Waves by Slightly Rough Surfaces, *IEEE Trans. Antennas Propagat.*, AP-15, 552-557, 1967.
12. Cox, C., and W. Munk, Measurement of the Roughness of the Sea Surface from Photographs of the Sun's Glitter, *J. Opt. Soc. Amer.*, 44, 838-850, 1954.

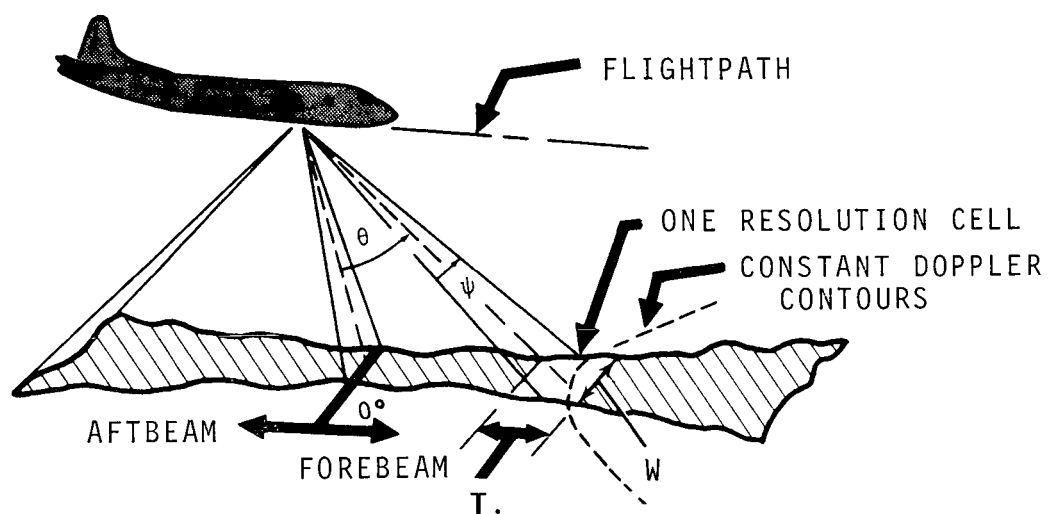


Figure 1. 13.3-GHz Scatterometer resolution cell geometry.

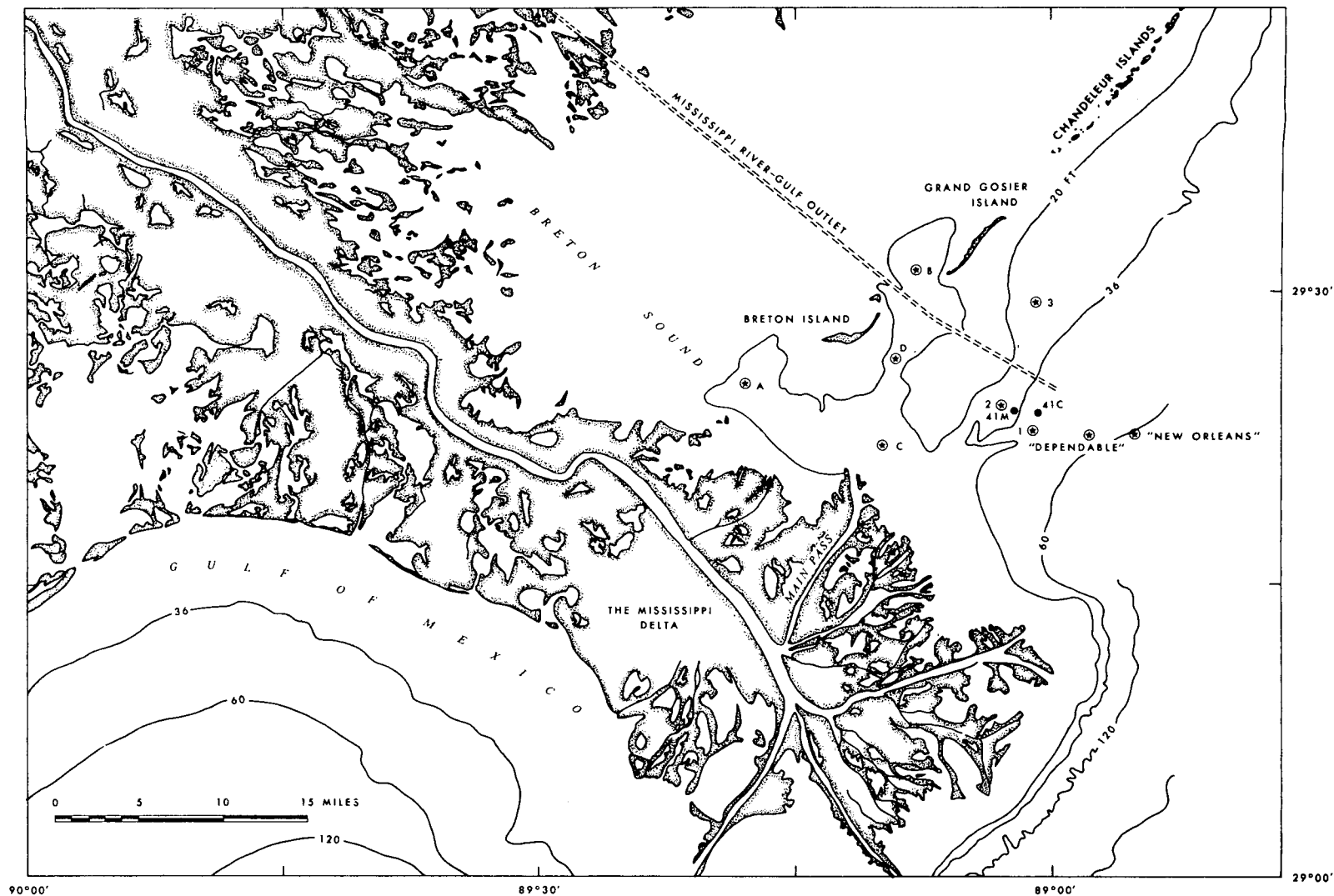


Figure 2. Location map showing stations occupied in study (from Murray et al, 1970).

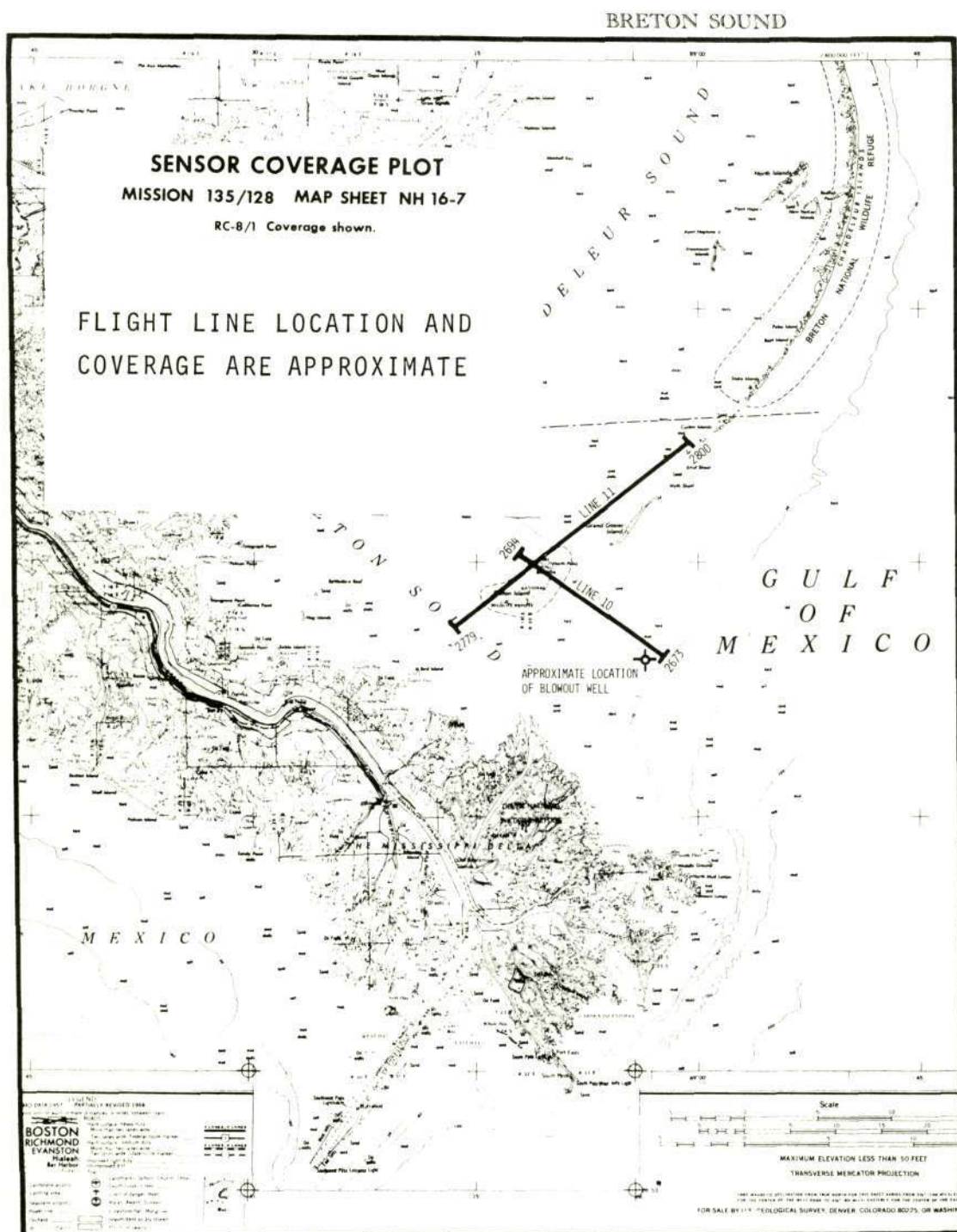


Figure 3. Approximate flight line location, from NASA/MSC Mission 135 Screening and Indexing Report (1970).

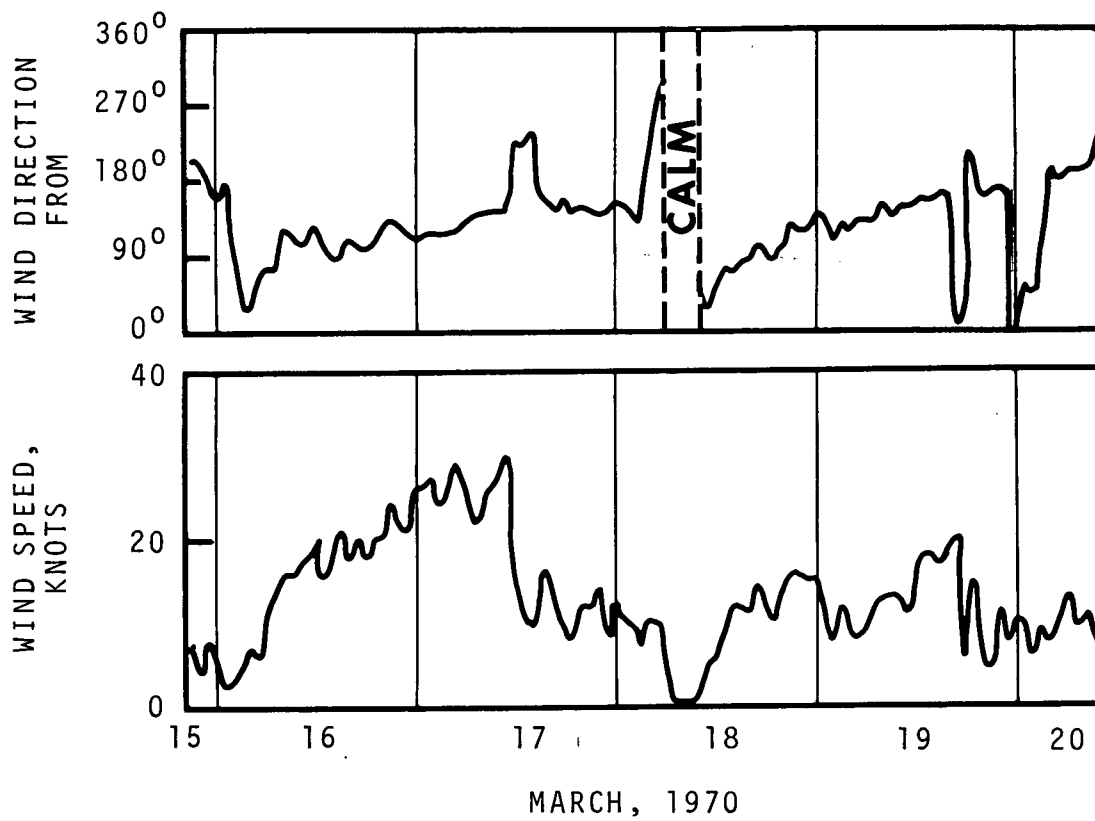


Figure 4. Wind speed and direction at *Dependable* station.

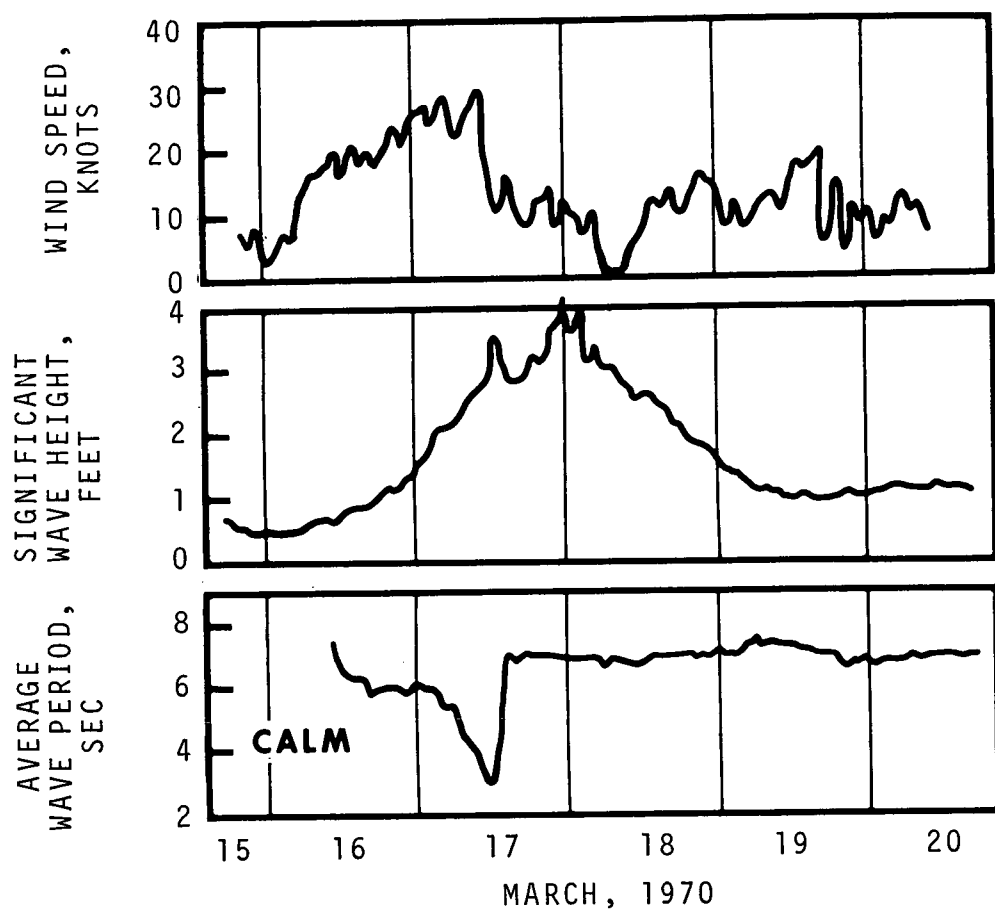


Figure 5. Wave height and wave period from 521 meter installed at Chevron platform MP-41M and wind speed for same intervals.

NORTH

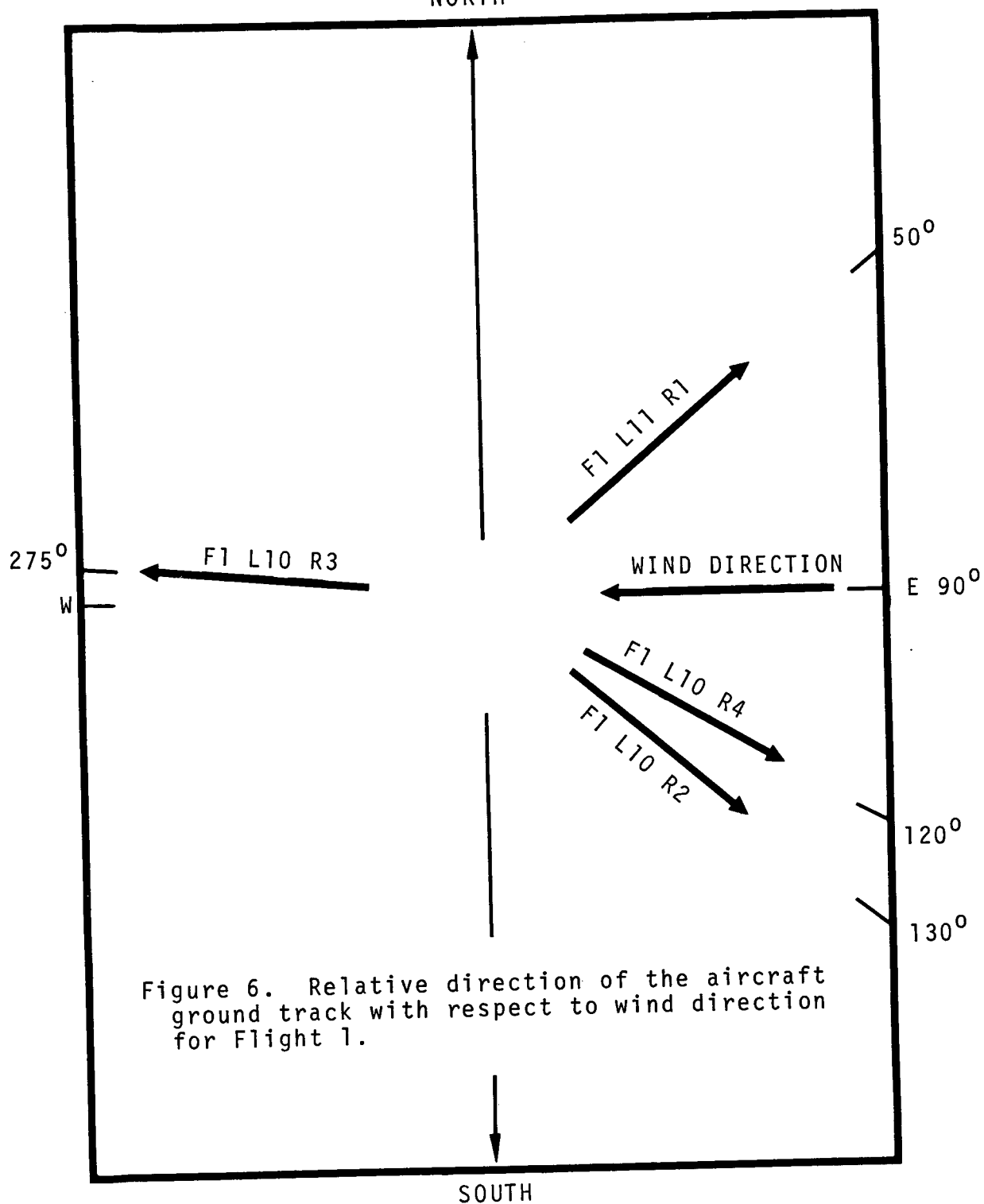


Figure 6. Relative direction of the aircraft ground track with respect to wind direction for Flight 1.

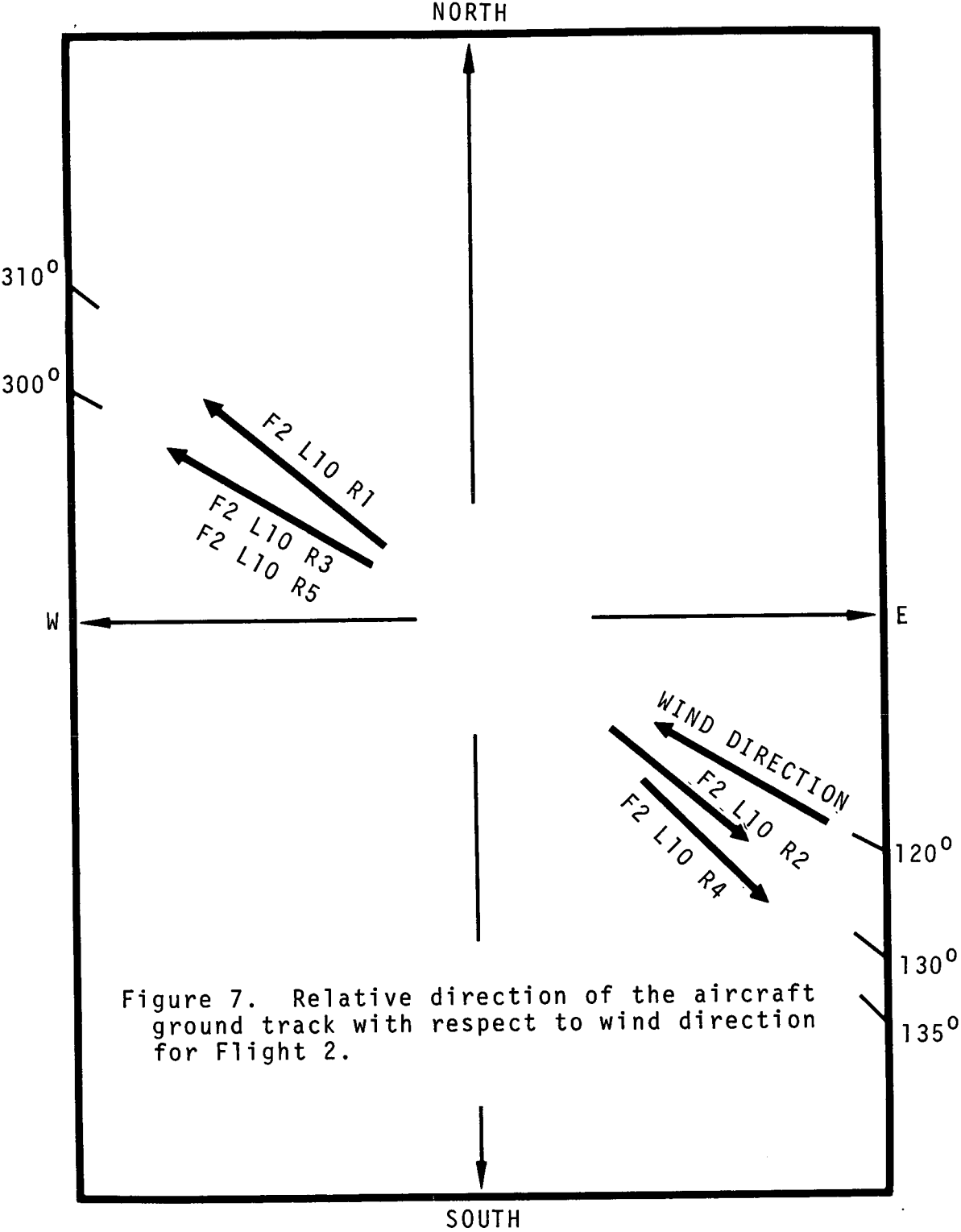


Figure 7. Relative direction of the aircraft ground track with respect to wind direction for Flight 2.

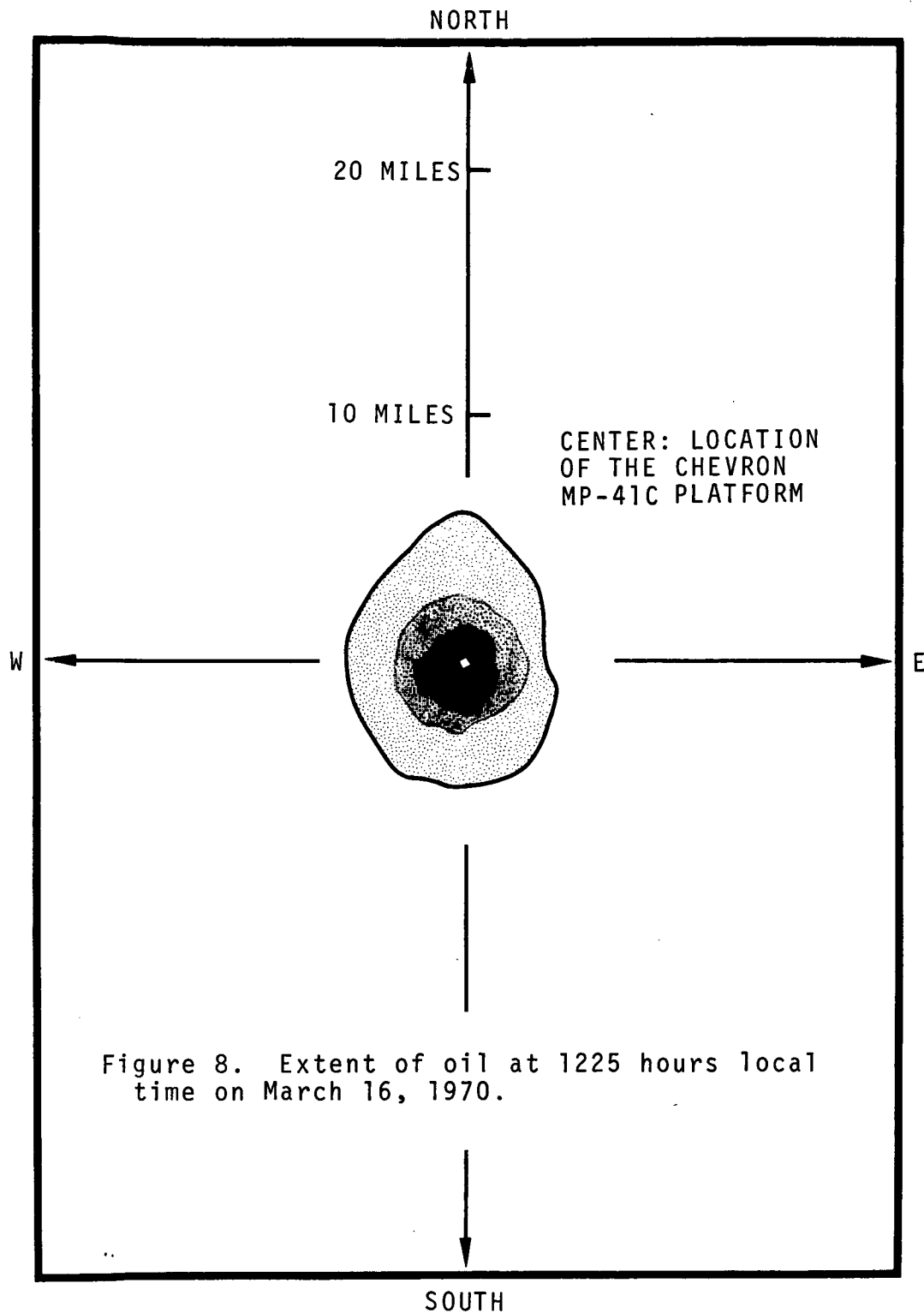




Figure 9. RC-8 photograph of Chevron MP-41C platform.



Figure 10. RC-8 photograph of an area with no significant oil slick.

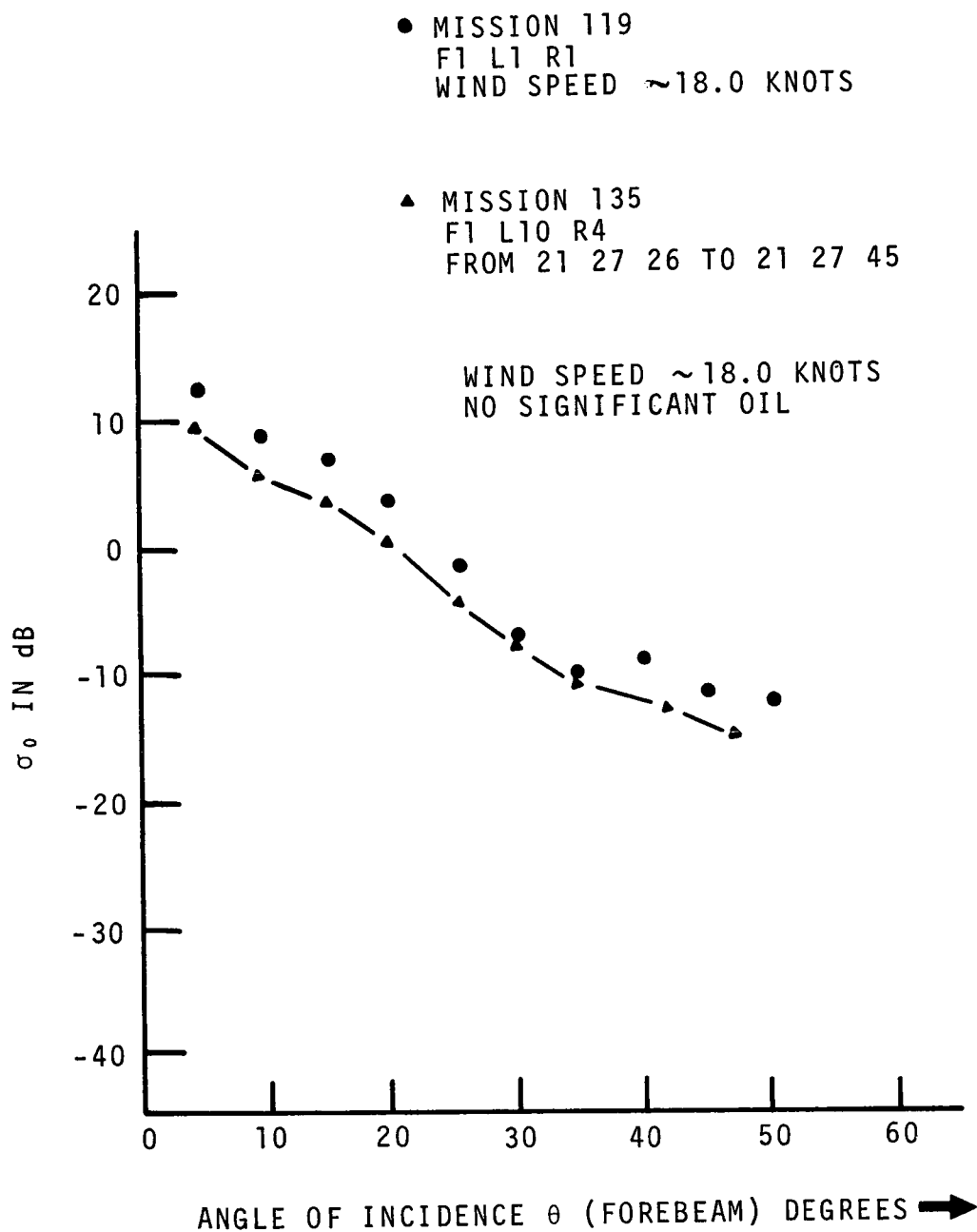


Figure 11. Comparison of Mission 135 data with Mission 119 data.



Figure 12. RC-8 photograph of an area with significant oil slick.

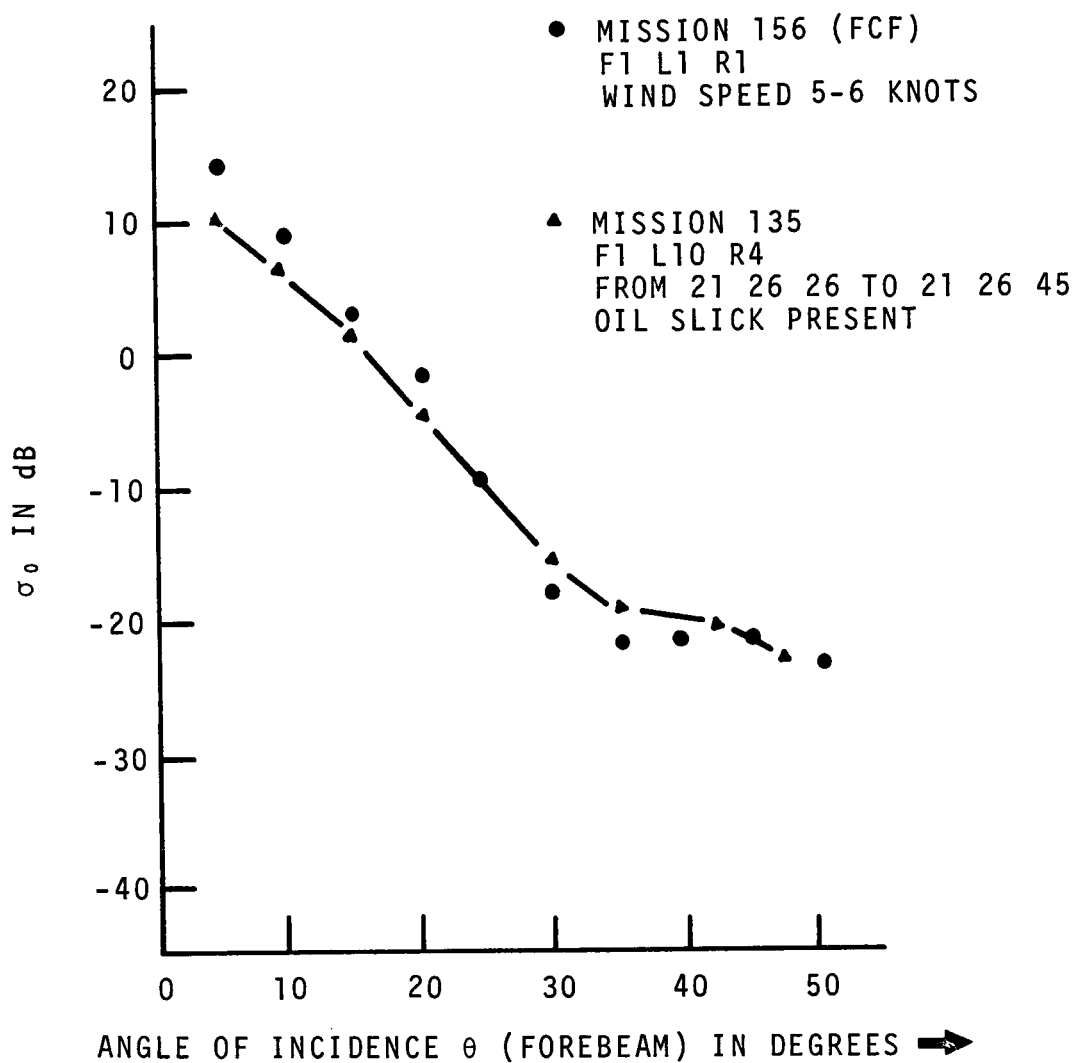


Figure 13. Comparison of Mission 135 data with Mission 156 (FCF) data.

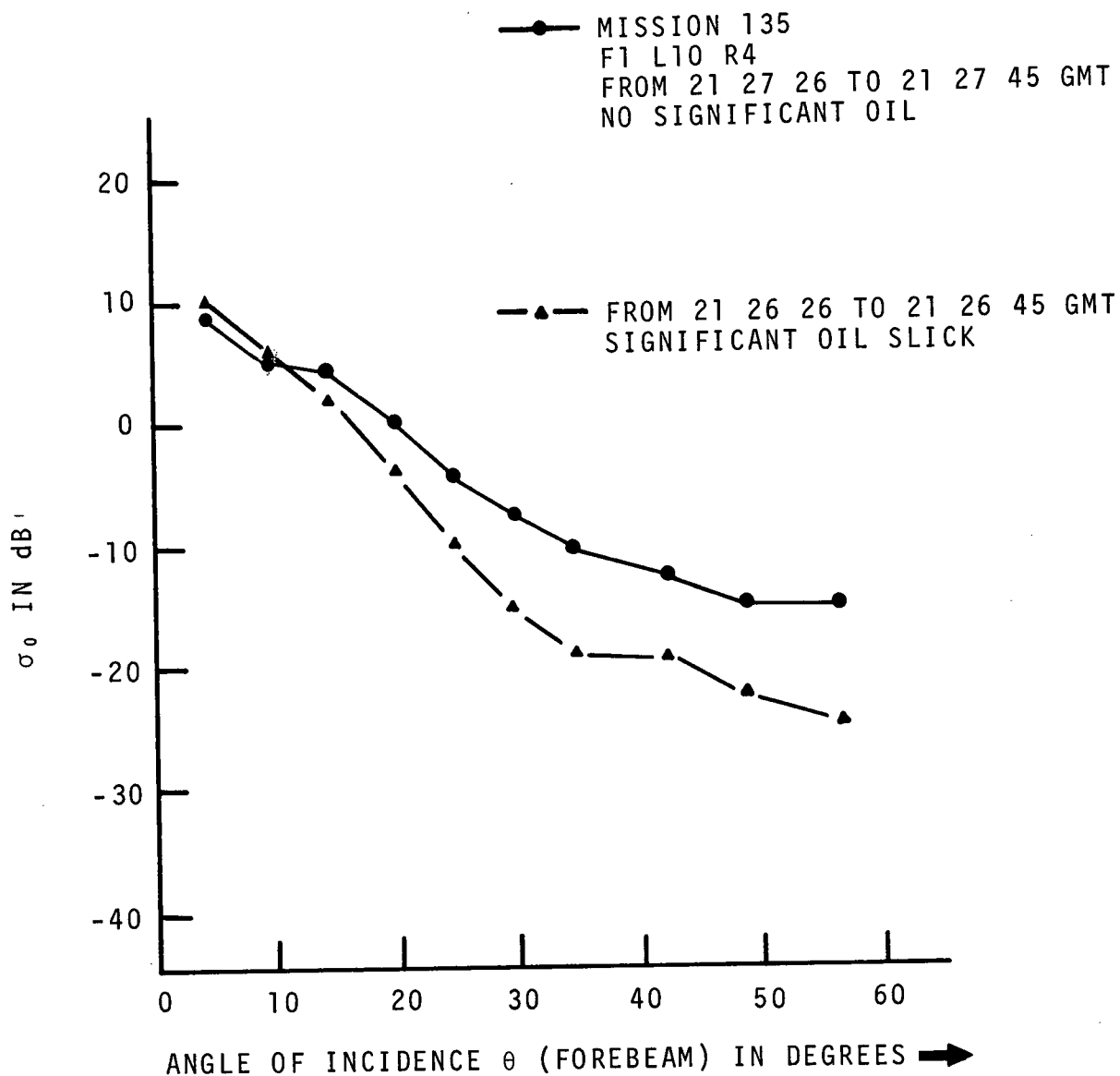


Figure 14. Comparison of scattering cross section of oil slick area and no significant oil slick area for flight 1.

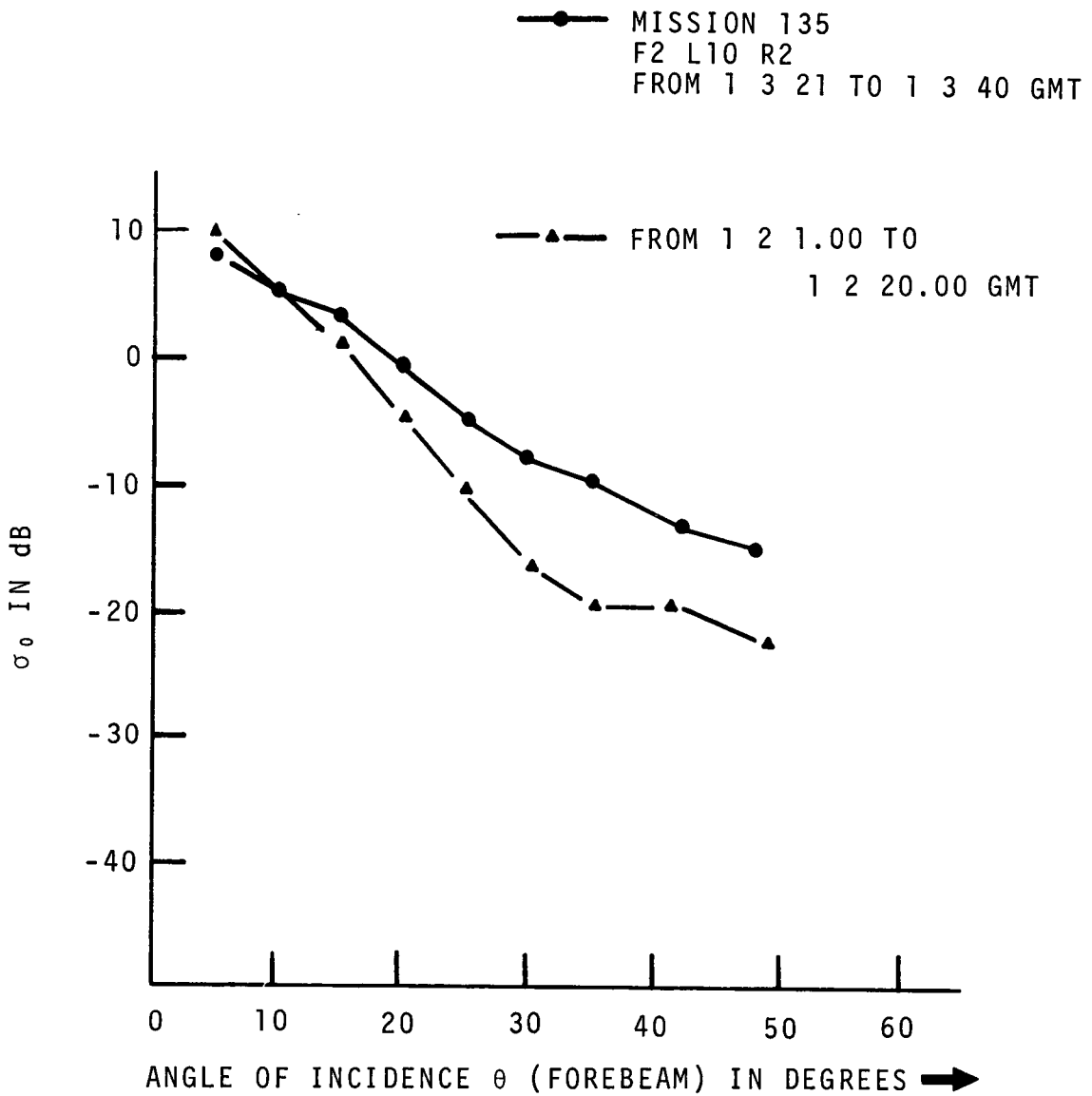


Figure 15. Comparison of $\sigma_0(\theta)_{dB}$ of oil slick and no significant oil slick data for flight 2.

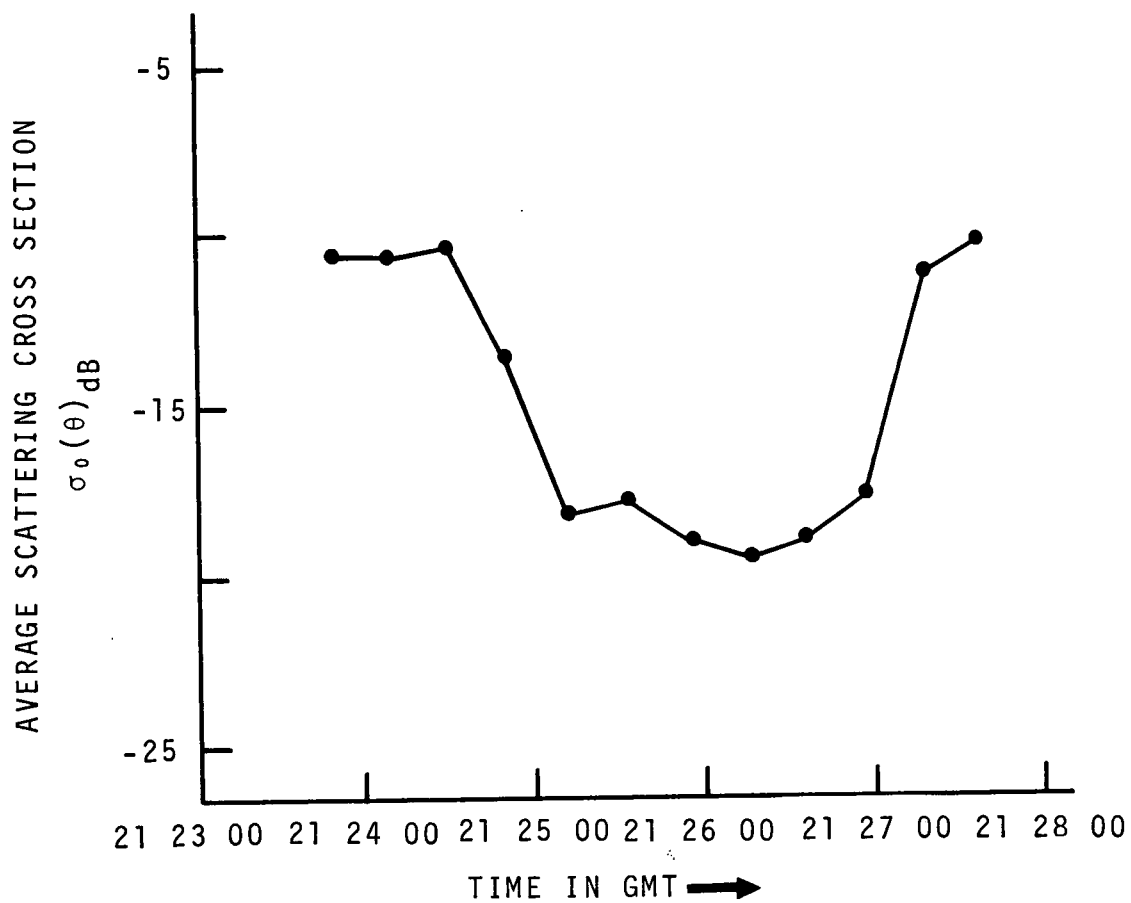


Figure 16. Average value of scattering cross section at $\theta = 35^\circ$ along ground track for F1 L10 R4.

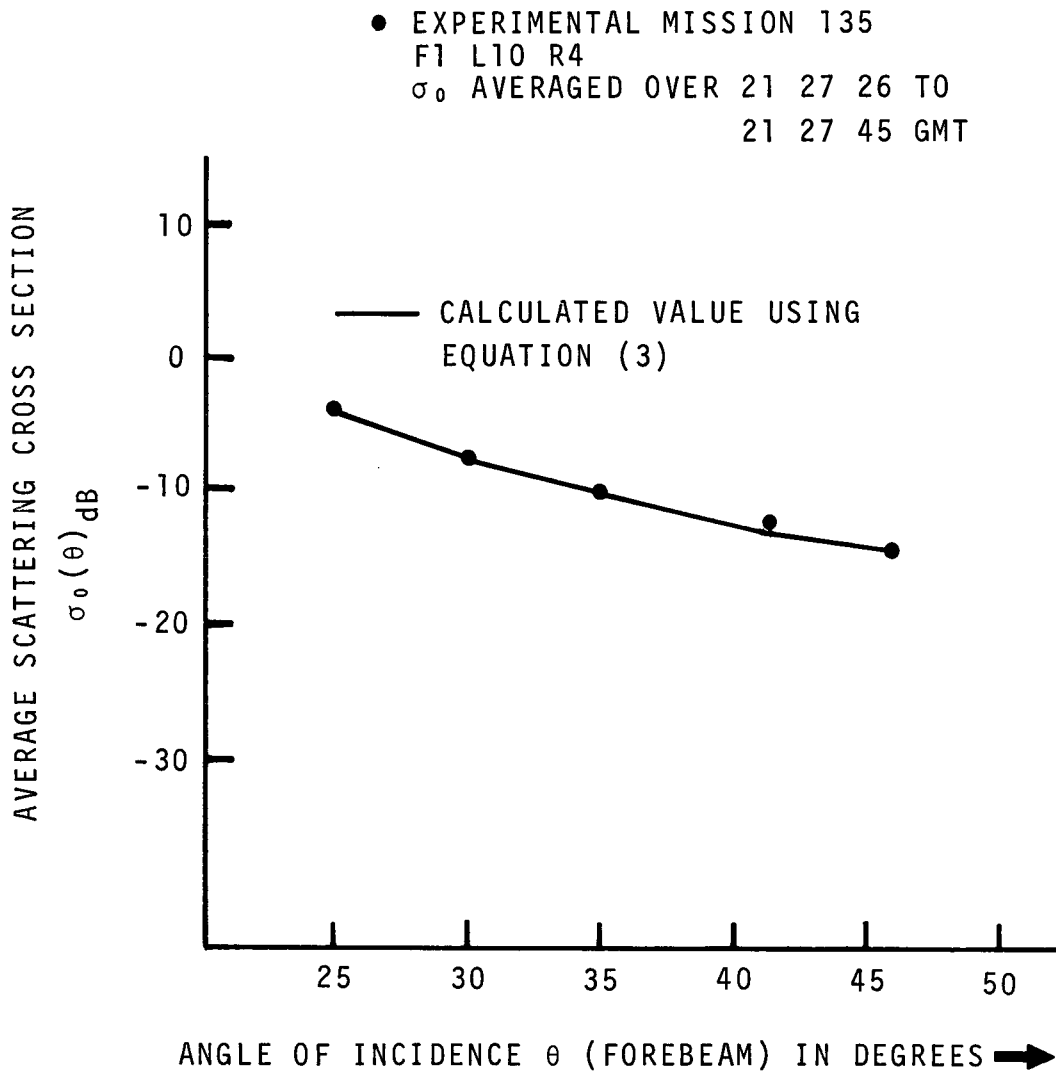


Figure 17. Comparison of calculated and experimental scattering cross section for Mission 135 (no significant oil present).

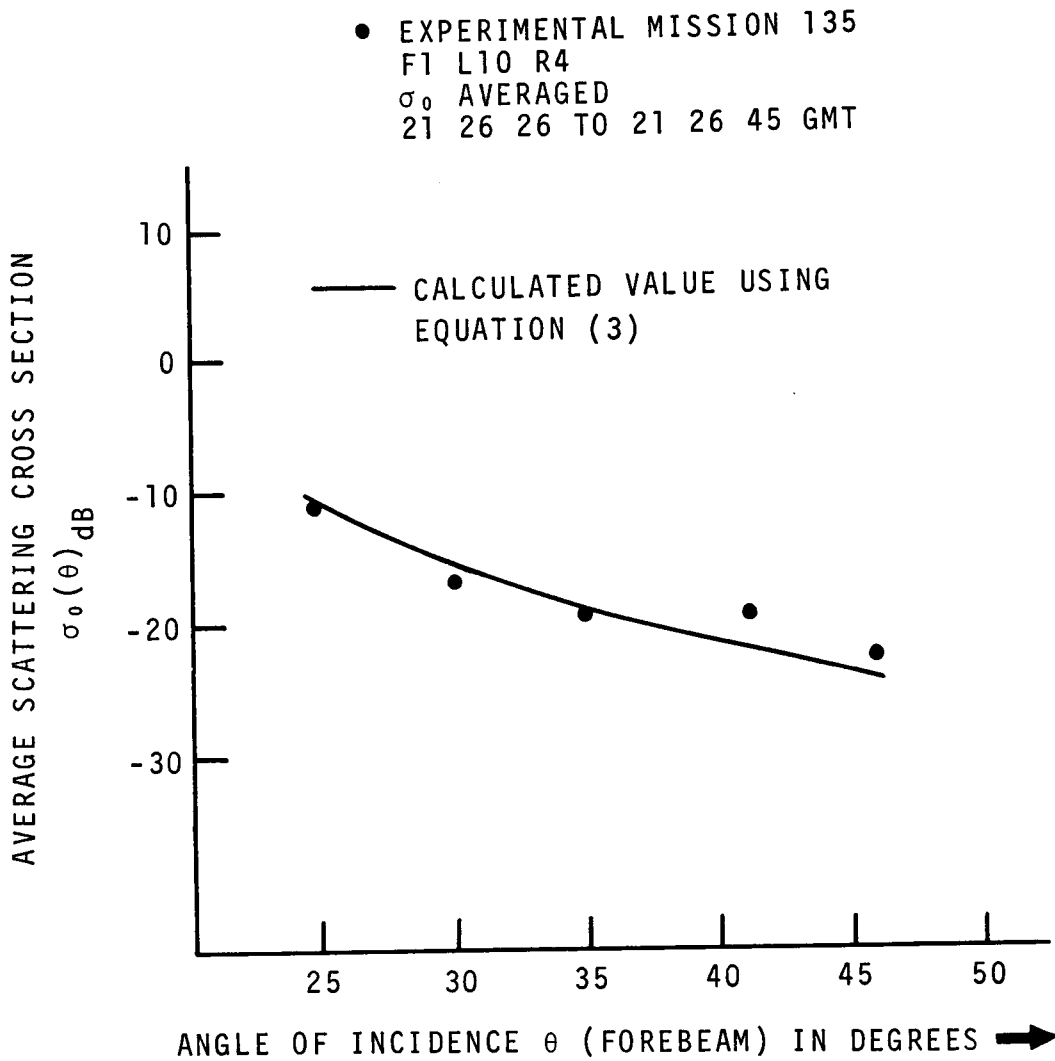


Figure 18. Comparison of calculated and experimental scattering cross section for Mission 135 (significant oil present).